Received: 28 October 2020 | Revised: 20 February 2021 | Accepted: 20 February 2021

DOI: 10.1111/cas.14868

ORIGINAL ARTICLE

Cancer Science WILEY

GPR126 regulates colorectal cancer cell proliferation by mediating HDAC2 and GLI2 expression

Hengxiang Cui[1,2] | Wenjie Yu[3] | Minhao Yu[5] | Yang Luo[5] | Mingming Yang[4] | Ruochen Cong[1] | Xin Chu[1] | Ganglong Gao[5] | Ming Zhong[5]

[1]Medical Research Center, Second Affiliated Hospital of Nantong University, Nantong, China

[2]Institute of Neuroscience, State Key Laboratory of Neuroscience, CAS Center for Excellence in Brain Science and Intelligence Technology, Chinese Academy of Sciences, Shanghai, China

[3]Department of Internal Medicine, Carver College of Medicine, The University of Iowa, Iowa City, IA, USA

[4]Department of Biochemistry and Molecular Biology, School of Medicine, Nantong University, Nantong, China

[5]Department of Gastrointestinal Surgery, School of Medicine, Renji Hospital, Shanghai Jiao Tong University, Shanghai, China

Correspondence
Hengxiang Cui, Medical Research Center, Second Affiliated Hospital of Nantong University, 6 North Hai'er Xiang Rd, Chongchuan District, Nantong 226001, Jiangsu, China.
Email: hengxiangc@qq.com

Ming Zhong, Department of Gastrointestinal Surgery, Renji Hospital, School of Medicine, Shanghai Jiao Tong University, 160 Pujian Rd, Shanghai 200127, Shanghai 200127, China.
Email: drzhongming@sjtu.edu.cn

Ganglong Gao, Department of Gastrointestinal Surgery, Renji Hospital, School of Medicine, Shanghai Jiao Tong University, 160 Pujian Rd, Shanghai 200127, Shanghai 200127, China.
Email: ggl149@126.com

Funding information
Science Fund for Research Initiation for Doctor of Second Affiliated Hospital of Nantong University, grants from the Nantong Municipal Bureau of Science and Technology, Grant/Award Number: MS12020001; National Natural Science Foundation of China, Grant/Award Number: 81874140 and 81873555; Nantong Municipal Health and Family planning commission, Grant/Award Number: M2020010; Shanghai Health and Family planning commission, Grant/Award Number: 201740141; Shanghai Municipal Commission

Abstract

The G-protein-coupled receptor 126 (GPR126) may play an important role in tumor development, although its role remains poorly understood. We found that GPR126 had higher expression in most colorectal cancer cell lines than in normal colon epithelial cell lines, and higher expression levels in colorectal cancer tissues than in normal adjacent colon tissues. GPR126 knockdown induced by shRNA inhibited cell viability and colony formation in HT-29, HCT116, and LoVo cells, decreased BrdU incorporation into newly synthesized proliferating HT-29 cells, led to an arrest of cell cycle progression at the G1 phase in HCT-116 and HT-29 cells, and suppressed tumorigenesis of HT-29, HCT116, and LoVo cells in nude mouse xenograft models. GPR126 knockdown engendered decreased transcription and translation of histone deacetylase 2 (HDAC2), previously implicated in the activation of GLI1 and GLI2 in the Hedgehog signaling pathway. Ectopic expression of HDAC2 in GPR126-silenced cells restored cell viability and proliferation, GLI2 luciferase reporter activity, partially recovered GLI2 expression, and reduced the cell cycle arrest. HDAC2 regulated GLI2 expression and, along with GLI2, it bound to the PTCH1 promoter, as evidenced by a chip assay with HT-29 cells. Purmorphamine, a hedgehog agonist, largely restored the cell viability and expression of GLI2 proteins in GPR126-silenced HT-29 cells, whereas GANT61, a hedgehog inhibitor, further enhanced the GPR126 knockdown-induced inhibitory effects. Our findings demonstrate that GPR126 regulates colorectal cancer cell proliferation by mediating the expression of HDAC2 and GLI2, therefore it may represent a suitable therapeutic target for colorectal cancer treatment.

Hengxiang Cui, Wenjie Yu, Minhao Yu contributed equally to this work.

of science and technology, Grant/Award Number: 19411966200

KEYWORDS

cell proliferation, colorectal cancer, GPR126, RNA-Seq, xenografts

1 | INTRODUCTION

The adhesion G protein-coupled receptor Gpr126 (Adgrg6) plays an important role in a variety of tissues. It regulates the initiation, maturation, and maintenance of the myelin sheath,[1-3] the process of arthrogryposis multiplex congenital [4] and vascular angiogenesis,[5] the development of the heart and inner ear,[6-8] and osteoblast differentiation and mineralization during embryonic bone formation.[9] Genome analysis revealed that Gpr126 regulates other important biological functions. A genetic variant of *GPR126* causing decreased inclusion of exon 6 was associated with cartilage development in an adolescent population with idiopathic scoliosis.[10] *GPR126* has also been associated with lung function in samples collected from Argentinean highlanders.[11] Through whole exome sequencing, a homozygous missense variation (c.3264G > C, p.W1088C) in *GPR126* was found to be associated with profound intellectual disability, severe speech impairment, microcephaly, and seizures during infancy.[12]

Mounting evidence indicates that *GPR126* may play an important role in tumors. In whole-genome sequences, a mutational hotspot in intron 6 of *GPR126* was identified in 2.7% of a large breast cancer series.[13] Copy number variation (CNV) profiling of genes in 59 breast cancer cell lines and 650 breast cancer patients showed that *GPR126* is associated with reduced patient survival.[14] Other aggregated whole-genome sequencing data from 2658 cancers across 38 tumor types showed that the *GPR126* enhancer is frequently mutated in transitional cell carcinoma of the bladder, and in breast adenocarcinoma.[15] In a cohort of patients with bladder cancers, including 44 nonmuscle invasive bladder cancers (NMIBC) and 59 muscle invasive bladder cancers (MIBC), somatic *GPR126* noncoding mutations occurred in 47.7% of samples, and were negatively associated with *GPR126* mRNA levels in NMIBCs, while somatic *GPR126* mutations occurred in 44.1% of MIBC samples. The *GPR126* intronic mutational hotspot is a promising clinical biomarker for monitoring tumor burden.[16] In another independent study, somatic mutations in the region of *GPR126/ADGRG6*, including two highly recurrent sites (chr. 6:142,706,206 G > A and chr. 6:142,706,209 C > T), located in the enhancer, were associated with enhanced protein expression in bladder cancer, and had poor prognosis. Functional assays demonstrated that a reduction of *GPR126/ADGRG6* expression in urothelial bladder carcinoma (UBC) cells compromises their ability to recruit endothelial cells and induce tube formation.[17] *GPR126/ADGRG6* also alters its function through fusion with other oncogenes. A patient with lung adenocarcinoma showing a ROS1-ADGRG6 rearrangement generated by the fusion of exons 1-33 of *ROS1* on chr6:q22.1 to exons 2-26 of *ADGRG6* on chr6:q24.2 was responsive to crizotinib.[18] GPR126 upregulation has also been reported in acute myeloid leukemia-affected patients suffering from variable mixed-lineage leukemia translocation, indicating its subtyping-specific tumorigenic role.[19]

Histone deacetylases (HDACs), particularly class I HDACs, including HDACI, HDAC2, and HDAC3, are frequently overexpressed in cancer, where they alter cellular epigenetic programming to promote cell proliferation and survival.[20-23] HDAC2 is upregulated in colorectal cancer compared with matched normal tissues, and regulates cell proliferation in human colorectal cancer.[20,24] Aberrantly activated Hedgehog (HH) signaling has been identified in the phenotypes of several types of human cancers,[25,26] involving amplification of GLI1 or GLI2. There is growing evidence that HH signaling drives cellular survival during colon carcinogenesis[25,27-29] and in metastatic disease.[28] GLI1 and GLI2, downstream of HH signaling, are transcriptionally enhanced by HDAC1- and HDAC2-mediated deacetylation, though common histone acetyltransferases (HATs) are activated, and HDACs repress transcription by modulating the acetylation status of histones or transcription factors.[30,31]

Few studies have revealed whether GPR126 plays a regulatory role in tumors of specific tissue origin or whether GPR126 regulates tumor growth. We evaluated the expression pattern of GPR126 in colorectal cancer cell lines and human tumor tissues, and found that GPR126 is highly enriched in these cells. We further found that *GPR126* regulates HDAC2 expression, as evidenced by RNA-Seq and subsequent immunoblotting of colorectal cancer cells. GPR126 knockdown decreased HDAC2 expression, resulting in GLI2 downregulation, regulating the proliferation of colorectal cancer cells in vitro and in vivo.

2 | MATERIALS AND METHODS

2.1 | Cell culture and lentivirus-based overexpression and knockdown

All colorectal cancer cell lines and FHC (CRL-1831), a normal human colon mucosal epithelial cell line, were obtained from the American Type Culture Collection (ATCC; Manassas, VA, USA) and maintained in the appropriate culture medium (Life Technologies, Carlsbad, CA, USA) supplemented with 10% fetal bovine serum (FBS) and 1% antibiotics (penicillin-streptomycin) at 37°C and 5% CO_2. NCM460 were purchased from Incell corporation (San Antonio, TX, USA). NCM460, HEK293T, HCT-116, HT-29, SW480, SW620, and FHC cell lines were maintained in DMEM medium containing high glucose; Caco-2 in MEM medium; HCT-8, HCT-15, and COLO 205 in PRIM1640 medium; and LoVo in DMEM-F12 medium. Lentiviruses were generated by transiently transfecting knockdown, overexpression, or control constructs, together with viral packaging vectors (psPAX2 and pMD2G) into HEK293T cells by calcium phosphate transfection.[32] Viruses were harvested from the supernatant 48 h post-transfection before being used to infect target cells (2×10^5) with 5×10^6 TCID50.

The cells were not used for subsequent experiments until they were selected by puromycin for 48 h with another culture for 24 h.

2.2 | Tissue samples, immunohistochemistry, and pathologist visual scoring

A tissue microarray (BC05118) comprising 100 paraffin-embedded tumor and matched normal mucosa samples surgically obtained from 50 human colorectal cancer patients was purchased from US Biomax, Inc. (Rockville, MD, USA). All study methods were approved by the ethics committee of the Second Affiliated Hospital of Nantong University (ID: 2021KT005).

Immunostaining was performed according to standard procedures. Staining was developed using DAB (brown precipitate). Rabbit polyclonal antibodies against GPR126 (cat.: ab75356; Abcam, Cambridge, UK) were used at a dilution of 1:500. Slides were counterstained with hematoxylin. Images were acquired using a DM 4000B photomicroscope (Leica, Wetzlar, Germany). Each tissue microarray spot was examined by a pathologist who assigned a score for GPR126 expression based on staining intensity as follows: score 0, no staining detected; 1, low; 2, moderate; 3, intense staining.[33,34]

2.3 | DNA construction

Lentiviral-mediated knockdown was conducted using the pLKO.1-TRC cloning vector. The sequences of shRNA oligos targeting human GPR126 were CCTATCTTACATCCAAATCTA (sh1) and GCTCATTCAGACAA-CTTCTAT (sh2), while that targeting HDAC2 was AAGCATCAGGATTCTGTTA. For lentiviral-mediated overexpression of GPR126 (NM_020455.5) and HDAC2 (NM_001527.3), the open reading frames of the two genes were subcloned into the pLVX-IRES-ZsGreen1 vector. GPR126 was subcloned into pLVX-IRES-ZsGreen1 at XhoI and SpeI, and HDAC2 at XhoI and XbaI sites. The direct PCR primer sequences used for the two constructs mentioned above are as follows. GPR126 forward: 5′-GGG-CTCGAGATGATGTTTCGCTCAGA TCG-3′ and reverse, 5′-GGGACTAGTTTAGCATGGGCC-AGTTT-TGAC A-3′; HDAC2 forward: 5′-GGCCTCGAGATGGCGTACAGTCAAGGAG-3′ and reverse, 5′-GCCTCTAGATCAGGGGTTGCTGAGCTGTTCTG-3′.

2.4 | Cell growth and colony formation assays

A modified CellTiter 96®Aq_{ueous} One Solution Proliferation Assay (Promega, Madison, WI, USA) was used, according to manufacturer's instructions. To assess cell viability, 2000 infected cells were plated onto 96-well plates in triplicate for 5 days. Then, 20 μL MTS was added and the absorbance, which is directly proportional to the number of viable cells in the cultures, was measured at 490 nm using a microplate reader. For the cell growth curve, infected cells were seeded in triplicate at 1×10^4 cells per well. Cells were harvested and counted at the indicated time points.

For anchorage-independent growth assays, infected cells were suspended in 0.35% agar with DMEM containing 10% FBS, and seeded in triplicate onto solidified 0.4% agar containing culture medium at 5000 cells per well in 35 mm plates. After 4-5 weeks, clones were stained with 0.005% crystal violet and photographed under a dissection microscope.

2.5 | RNA isolation and qRT-PCR

Total RNA was extracted from cells using the TRIzol reagent (Invitrogen, Carlsbad, CA, USA). For first-strand cDNA synthesis, 1 μg of total RNA was reverse-transcribed in a 20 μL reaction using the PrimeScript RT Reagent Kits (Takara Bio, Kusatsu, Japan). cDNA samples were amplified in triplicate via qRT-PCR using the MxPro-Mx3005P Real-Time PCR system (Agilent Technologies, Santa Clara, CA, USA) and SYBR Premix Ex Taq (Takara Bio) according to the manufacturer's instructions. All primers used are listed in Table S1. The qRT-PCR cycling conditions were the following: initial denaturation at 95°C for 1 min, 95°C for 35 s, and annealing at 60°C for 35 s for 40 cycles. The $2^{-\Delta\Delta CT}$ method, with *β-actin* as internal control, was used to determine the relative expression. The fluorescent signals were measured after each primer-annealing step at 60°C.

2.6 | Digital gene expression library sequencing

Digital gene expression analysis (DGE; contract ID: HSZ11660) was supported by Huada Gene Company, Shenzhen, China (http://en.genomics.cn/navigation/index.action). Two DGE libraries for sequencing were generated by the Huada Gene Company from the total RNA of HT-29 cells infected with control vector or GPR126 sh1. The libraries were sequenced using Illumina technology with minor modifications,[35] in which each tunnel generated millions of raw reads with a sequencing length of 49 bps. The sequencing quality evaluation of the RNA-Seq analysis was conducted according to the tag distribution of each group. Gene Ontology annotation analysis and Kyoto Encyclopedia of Genes and Genomes (KEGG) pathway analyses were performed by the Huada Gene Company for functional annotation of the differentially expressed genes.

2.7 | Xenograft experiments

All animal experiments conformed to the regulations drafted by the Association for Assessment and Accreditation of Laboratory Animal Care in Shanghai, and were approved by the East China Normal University Center for Animal Research. Xenograft experiments were conducted in the East China Normal University Center for Animal Research, during which the infected HT-29, HCT-116, and LoVo cells were stereotactically implanted in the left (vector control) or right (shRNA) putamen region in the same nude

mouse; 15 nude mice were injected with 8.0×10^6 HT-29 cells resuspended in PBS, 10 nude mice were injected with 5.0×10^6 HCT-116, and eight nude mice were injected with 8.0×10^6 LoVo cells re-suspended in PBS. Tumor size was measured using calipers at the indicated time points from 4 to 6 weeks. Tumor volume was calculated using the formula $V = (L \times W^2) \times 0.52$, where L is the length and W is the width of the xenograft. Finally, mice were sacrificed and the xenografts were isolated, photographed, and frozen in liquid nitrogen for preservation.

2.8 | Western blot analysis

Cells were lysed in lysis buffer for 2 h on ice. Confluent cell layers were washed with PBS and lysed for 30 min at 4°C with 1% Nonidet P-40, 0.1% Triton X-100, 30 mM sodium phosphate (pH 7.4) containing 1 mM sodium orthovanadate, 2.5 mM Tris-HCl (pH 7.5), 100 mM NaCl, and 10 μg/mL leupeptin, aprotinin. Following centrifugation at 13,000 × *g* for 20 min at 4°C, the supernatant was collected. Protein concentration was measured using the Lowry protein assay. Total cell lysates (20-80 μg protein) were separated by 10% polyacrylamide gel electrophoresis and electro-transferred to a polyvinylidene fluoride membrane. The membrane was blocked by incubation with 5% nonfat milk powder in TBST for 2 h at 37°C before incubation with primary antibodies at 4°C overnight. The antibodies used were anti-GPR126 (ab75356; Abcam), anti-HDAC1 (H6287; Sigma-Aldrich, St. Louis, MO, USA), anti-HDAC2 (H2663; Sigma-Aldrich), anti-E2F2 (E8776; Sigma-Aldrich), anti-SIRT1 (ab32441; Abcam), anti-GLI1 (sc-20687; Santa Cruz Biotechnology, Dallas, TX, USA), anti-GLI2 (sc-271786; Santa Cruz Biotechnology), and β-actin (A5441; Sigma-Aldrich). Specific peroxidase-conjugated secondary antibodies or IRDye 800CW conjugated goat (polyclonal) anti-mouse (or rabbit) IgGs (ab216772 and ab216773; Abcam) were used for protein detection using an enhanced chemiluminescence kit (Pierce; Thermo Fisher Scientific, Waltham, MA, USA) or the Odyssey infrared imaging system (LI-COR Biosciences, Lincoln, NE, USA), respectively. The ECL signals were digitized using ImageJ software (v1.50i) (US National Institutes of Health, Bethesda, MD, USA).

2.9 | Cell cycle analysis

Infected cells were cultured for several days at a confluence of less than 80%. Cells were harvested and suspended in 1X PBS and fixed with cold ethanol at a final concentration of 70%. The cells were then stained with 50 mg/mL propidium iodide (Sigma-Aldrich) followed by RNase A (Sigma-Aldrich) treatment for 30 min at room temperature. DNA content was analyzed using a FACScan cell analyzer (BD Biosciences, San Jose, CA, USA) equipped with CellQuest software (BD Biosciences). Finally, the cell population in each cell cycle phase was determined.

2.10 | BrdU incorporation assays

BrdU incorporation assays were conducted as described previously.[36] The infected cells were incubated in the presence of 10 mM BrdU (Sigma-Aldrich) for 10 h, after starvation overnight. Cells were then fixed with 4% paraformaldehyde before treatment with 2 M HCl containing 1% Triton X-100. The cells were stained with monoclonal anti-BrdU (Sigma-Aldrich) antibody, followed by TRITC-conjugated goat anti-mouse antibodies and counterstaining with DAPI. The total numbers of GFP-positive as well as BrdU-labeled cells were counted in 8-10 different fields for each well.

2.11 | ChIP and re-chip assay

ChIP was performed as previously described.[37] HT-29 cells were grown in 100 cm tissue culture plates in DMEM for 2 days. Formaldehyde was added to the medium at a final concentration of 1%, and the reaction was incubated at room temperature with shaking for 10 min before glycine (0.125 M) was added. The reaction was then incubated for another 10 min. The media were removed before the cells were washed twice with cold PBS and 1 mM phenylmethylsulfonyl fluoride, scraped, collected by centrifugation, and lysed in SDS lysis buffer containing 1 mM phenylmethylsulfonyl fluoride, 1 mg/mL aprotinin, and 1 mg/mL pepstatin A. DNA was sheared to fragments of 500-1000 bp by 10 8-s sonication rounds. The chromatin was precleared with salmon sperm DNA/protein A-agarose slurry (Upstate Biotechnology, New York, NY, USA) for 1 h at 4°C with gentle agitation. The agarose beads were pelleted, and the precleared supernatant was incubated without (control anti-serum) or with anti-HDAC2 antibody (HDAC2 Ab) overnight at 4°C. For ReChIP, the agarose beads were pelleted to obtain chromatin immunocomplexes before elution with 10 mM DTT then a second round of immunoprecipitation with control anti-serum or specific GLI2 antibodies. The agarose beads were subsequently pelleted and washed with low-salt wash buffer [0.1% SDS, 1% Triton X-100, 2 mM EDTA, 20 mM Tris (pH 8.1), and 150 mM NaCl], high-salt wash buffer [0.1% SDS, 1% Triton X-100, 2 mM EDTA, 20 mM Tris (pH 8.1), and 500 mM NaCl], LiCl wash buffer [0.25 m LiCl, 1% IGEPAL CA-630, 1% deoxycholate, 1 mM EDTA, and 10 mM Tris (pH 8.1)], and twice in TE buffer [10 mM Tris-HCl (pH 8.0), and 1 mM EDTA]. After reversing the protein/DNA cross-links, DNA was recovered by phenol/chloroform extraction and ethanol precipitation. Eluted DNA was analyzed using standard PCR techniques. The oligonucleotides used for PCR amplification were as follows: PTCH1 promoter forward, 5′-CTCTGAGAGCGCCAACCTTC-3′ and reverse, 5′-GTCTACCGCGAGGCAAATG-3′; GAPDH control forward, 5′-CGGGATTGTCTGCCCTAATTAT-3′ and reverse, 5′-GCACGGAAGGTCACGATGT-3′. After PCR, the products were resolved on a 2.0% agarose gel and stained with ethidium bromide. Samples were visualized under UV light. The PCR products were purified and sequenced.

2.12 | Transfections and luciferase reporter assay

The reporter gene construct was prepared as previously described.[38] Briefly, the genomic DNA was extracted from HT-29 cells before being used to PCR amplify the fragment of the human GLI2 promoter which were from the −1624 position to the +367 transcriptional site in the GLI2 genomic promoter region, using BglII-containing forward primers and a HindIII-containing reverse primer as forward, 5′-GG GAGATCTGTGGAATGGCTGGAAGAGGGGGAGT-3′; reverse, 5′-G GGAAGCTTCTAGTTTGGAGCTGAAGTTG-3′. The PCR products containing the human GLI2 promoter were subcloned into pGL3-Basic vector (Promega) and sequenced, obtaining the pGL3-GLI2-Luc vector. Twenty-four hours prior to transfection, control virus (NC) or GPR126-Sh1 virus (Sh1) infected HT-29 cells were plated in 24-well plates and in the following day transfected with luciferase vectors (200 ng) with or without 50 ng of HDAC2 expressing vector (when necessary) using Lipofectamine LTX® Reagent (ThermoFisher). Forty nanograms of phRLMLP Renilla luciferase expression vector was co-transfected to evaluate transfection efficiencies. Twenty-four hours post-transfection, cells were lysed, and luciferase activity was determined with the Dual Luciferase reporter assay system (Promega). In each experiment, the promoter activity was expressed as the firefly/Renilla ratio relative to internal control conditions.

2.13 | Statistical analysis

Data are presented as the mean ± standard error of the mean (SEM). All statistical analyses were done using Prism 8 (GraphPad Software, San Diego, CA, USA). Unless otherwise mentioned, Student's t-tests were used for comparisons, and P values <.05 were considered significant.

3 | RESULTS

3.1 | GPR126 is enriched in colorectal cancer cell lines and clinical tissues

Because GPR126 expression is associated with the survival of patients with breast cancer and bladder cancer,[14,16,17] we hypothesized that GPR126 may also play a role in other tumors, such as colorectal cancer. We first evaluated the expression pattern of GPR126 in colorectal cancer by examining *GPR126* mRNA and protein levels in a few colorectal cancer cell lines. *GPR126* mRNA was differentially expressed, with considerable abundance in most human colorectal cancer cell lines, and was especially highly enriched in HCT-116, HT-29, and Caco-2 cells (Figure 1A) compared to the normal human colon mucosal epithelial cell lines, such as NCM 460 and FHC cells. GPR126 protein levels were higher in eight of nine colorectal cancer cell lines than in NCM 460 and FHC cells (Figure 1A). This difference between mRNA and protein expression may result from translation regulation; nevertheless, *GPR126* was highly enriched in colorectal cancer cell lines.

Using the human colorectal cancer tissue microarray, we further found that GPR126 protein levels were higher in most colorectal cancer tissues than in the paired normal mucosa tissue (Figure 1B). To assess this increase quantitatively, GPR126 staining intensity in the tissue microarrays was graded and scored according to

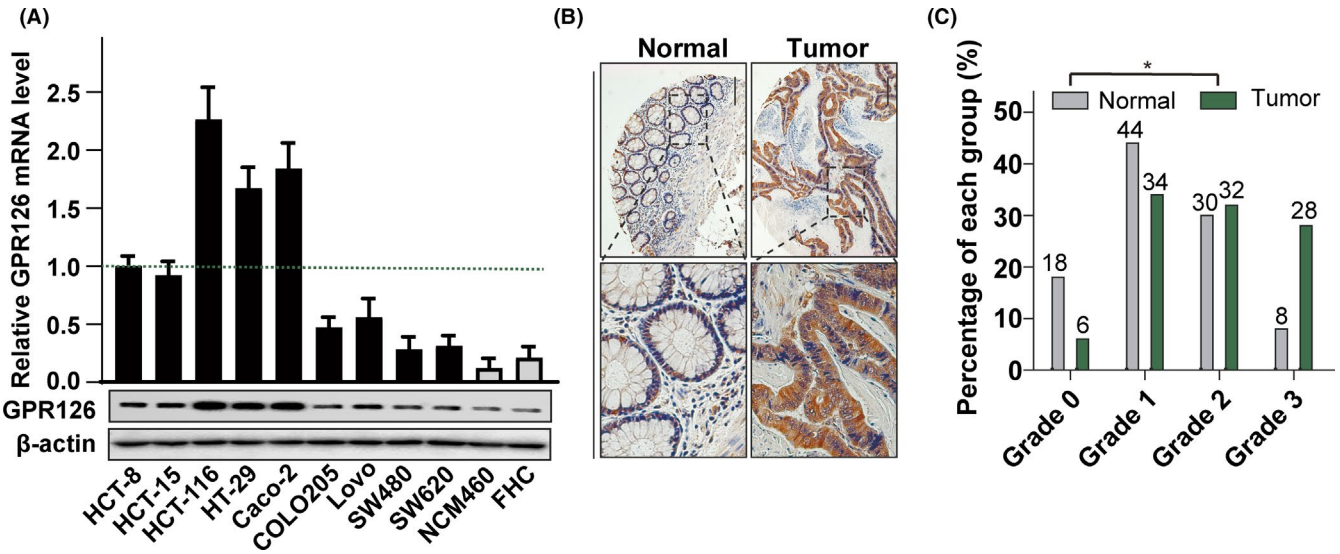

FIGURE 1 GPR126 is enriched in colorectal cancer cell lines and clinical colorectal cancer tissues. A, Relative *GPR126* mRNA and protein expression levels evaluated by qRT-PCR and western blotting, with the β-actin as the internal control, in the indicated colorectal cancer cell lines. B, Representative immunohistochemistry staining of GPR126 (brown) in matched human colorectal cancer tissue and adjacent normal tissue. Scale bar = 50 μm. C, Statistical analysis of immunohistochemistry staining scores of GPR126 from 50 pairs of human colorectal cancer tissue (green) and matched adjacent normal colorectal tissue (grey) in the tissue microarray. The number on each column top represents the percentage of tissues per indicated grade. Chi square test was used for comparisons. *, P <.05

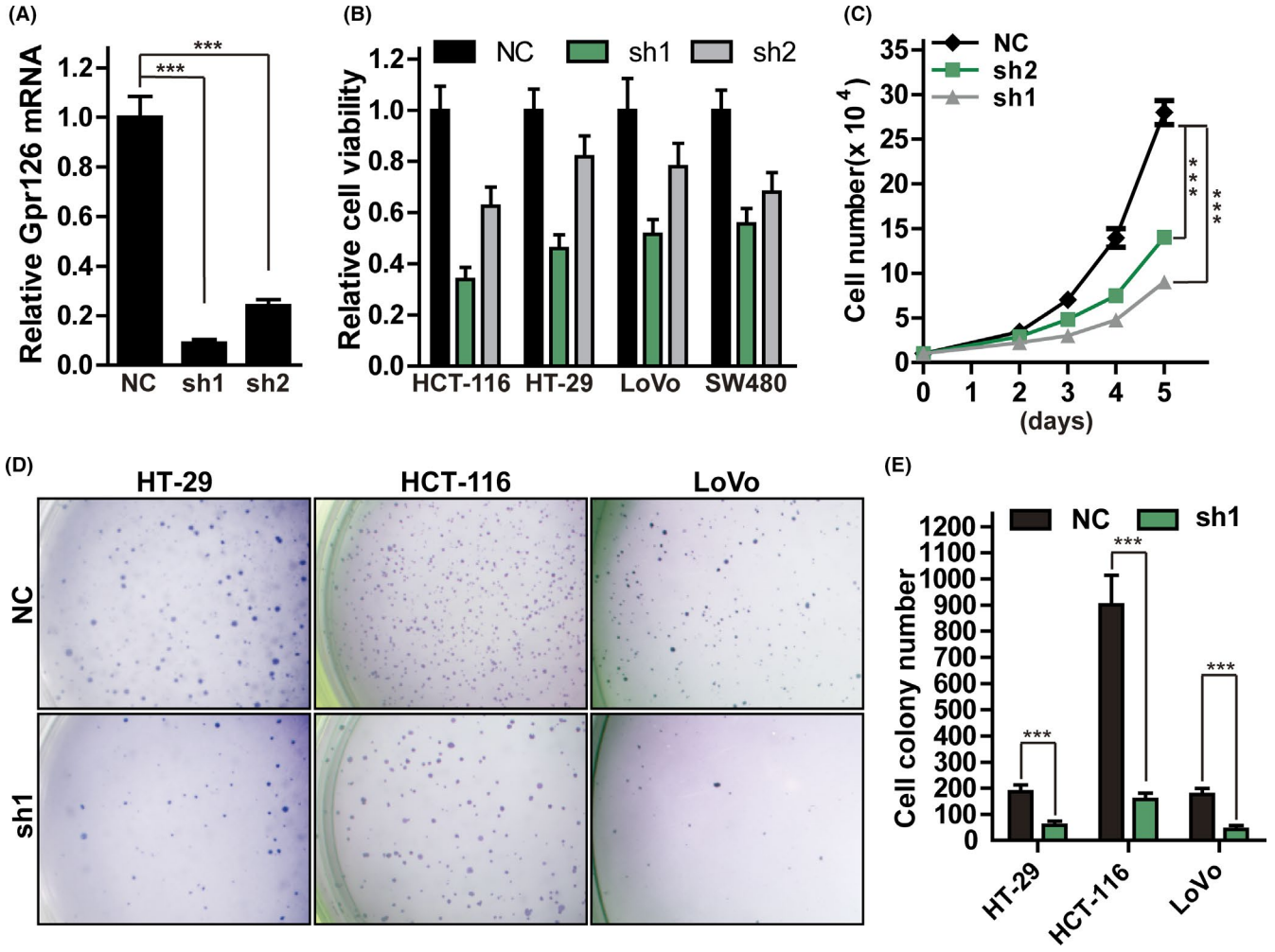

FIGURE 2 GPR126 knockdown attenuates colorectal cancer cell growth in vitro. A-C, Cell viability and growth of the indicated cells after GPR126 knockdown. The effect of two shRNAs targeting GPR126 (sh1, sh2) on GPR126 mRNA expression normalized to β-actin mRNA in HT-29 cells (A), cell viability of the indicated cells (B), and the growth of HT-29 cells (C). NC, control vector. D, E, Cell colony formation in soft agar after shRNA (sh1)-mediated GPR126 knockdown. NC, control vector. Representative images of the stained cell colonies (triplicate plates for each indicated cell line were used) (D). Quantification of cell colony numbers in (D) represented as a bar plot (E). Values are presented as the mean ± SEM. ***P <.001

representative images of the GPR126 expression pattern, as shown in Figure S1. The result was summarized as a percentage of each grade according to tissue type. The percentage of colorectal cancer tissue samples with grade 0 was 6% (3/50), which is less than the 18% (9/50) of the adjacent mucosal tissue group (Figure 1C); 34% (17/50) of colorectal cancer tissues and 44% (22/50) of the adjacent mucosal tissues were grade 1, while 32% (16/50) of colorectal cancer tissues and 30% (15/50) of the adjacent mucosal tissues were grade 2 (Figure 1C). Finally, 28% (14/50) of colorectal cancer tissues and only 4% (2/50) of the adjacent mucosal tissue group were grade 3 (Figure 1C). Compared with the adjacent mucosal tissues, more colorectal cancer tissues were grade 3, and fewer were grade 0. Using Chi-square tests, we found that there was a significant difference in GPR126 expression between adjacent mucosal tissues and colorectal cancer tissues (Figure 1C). GPR126 proteins were enriched in colorectal cancer tissues, as evidenced by the cancer tissue microarray.

3.2 | GPR126 knockdown attenuates colorectal cancer cell growth in vitro and in vivo

Given that GPR126 was highly expressed in colorectal cancer cell lines and in some colorectal cancer tissues (Figure 1), we theorized that GPR126 may regulate colorectal cancer growth. We first generated two shRNAs, sh1 and sh2, targeting GPR126. qRT-PCR analysis of *GPR126* mRNA in HT-29 cells. We showed that GPR126 was successfully silenced by shRNAs, with sh1 having a strong knockdown effect on mRNA and protein expression (Figures 2A and S2C). We evaluated the effect of GPR126 knockdown on cell proliferation in nine colorectal cancer cells, including HCT-15, SW620, LoVo, HCT-8, HT-29, Caco-2, SW480, COLO205, and HCT-116 cells. Silencing GPR126 in these cell lines attenuated cell viability (Figures S2A and S2B), notably inhibiting HCT-116 and COLO 205 cell viability (Figures S2A and 2B). We further confirmed that GPR126 knockdown using two shRNAs in HCT-116, HT-29, LoVo, and SW480 cells

significantly attenuated cell viability (Figures 2B and S2C). A cell growth assay was also carried out using HT-29 cells infected with scramble shRNA virus or GPR126 shRNA virus; 1000 cells per treatment were cultured and counted daily over 5 days. Cell counts of the sh1 and sh2 groups were significantly lower than those of the scramble group (NC) (Figures 2C and S2C). The ability to form colonies in soft agar was also assessed in HT-29, HCT116, and LoVo cells, in which GPR126 knockdown significantly reduced the number of colonies (Figure 2D, 2E and S2C).

To evaluate the role of GPR126 in modulating the growth of colorectal cancer cells in vivo, we established xenograft mouse models by transplanting cancer cells infected with either scramble shRNA (NC) or GPR126-sh1. NC- and GPR126-sh1-infected colorectal cancer cells were injected into the right and left flanks of nude mice, respectively (Figure S3). Tumors were measured every 5 days starting from day 7, and harvested approximately 1 month after injection. As shown in Figure 3A, GPR126 knockdown in HCT-116 cells significantly attenuated tumor growth (n = 10) by day 29. GPR126 knockdown in HT-29 (n = 15) and LoVo (n = 10) also significantly suppressed tumor volume by days 27 and 35, respectively (Figure 3B,C). Thus, our findings indicate that GPR126 knockdown inhibits colorectal cancer cell growth in vitro and in vivo.

3.3 | GPR126 knockdown leads to DNA synthesis inhibition and G1 phase cell cycle arrest

To investigate whether this growth inhibition effect mediated by GPR126 knockdown is a consequence of apoptosis, we stained cancer cells with annexin V and performed FACS analysis. The ratio of cell apoptosis was not affected by GPR126 knockdown in HT-29 and SW480 cells (Figure S4B). Subsequently, we conducted BrdU incorporation assays using NC- and GPR126-sh1-infected colorectal cancer cells to further assess the GPR126 regulation of cell proliferation. GPR126 knockdown significantly reduced the number of BrdU-positive cells (Figures 4A,B and S4A), suggesting that GPR126 promotes cell proliferation by regulating DNA synthesis. Next, we examined cell cycle progression in GPR126-knockdown HCT-116 and HT-29 cells using FACS analysis. *GPR126*-knockdown HCT-116 and HT-29 cells accumulated in the G1 phase at a percentage of 56.62 ± 3.12% and 62.09 ± 2.89% compared with 41.03 ± 2.17% and 47.98 ± 2.36% in the NC group, respectively (Figure 4C). In both HCT-116 and HT-29 cells, GPR126 knockdown reduced the percentage of cells in the S phase (Figure 4C).

Based on the results of the BrdU incorporation assays and FACS, we can conclude that GPR126 knockdown leads to cell cycle arrest in the G1 phase, resulting in DNA synthesis inhibition and attenuating HCT-116 and HT-29 cell proliferation.

3.4 | GPR126 knockdown decreases DNA synthesis and expression of cell cycle-related genes

To further investigate the mechanism by which GPR126 regulates colorectal cell proliferation, we performed RNA-Seq profiling of HT-29 cells, comparing GPR126 knockdown cells to control cells. We generated 5,753,320 and 6,010,192 clean reads, reaching a total tag ratio of 96.22% and 96.28% with an average mapping ratio to reference gene and genome

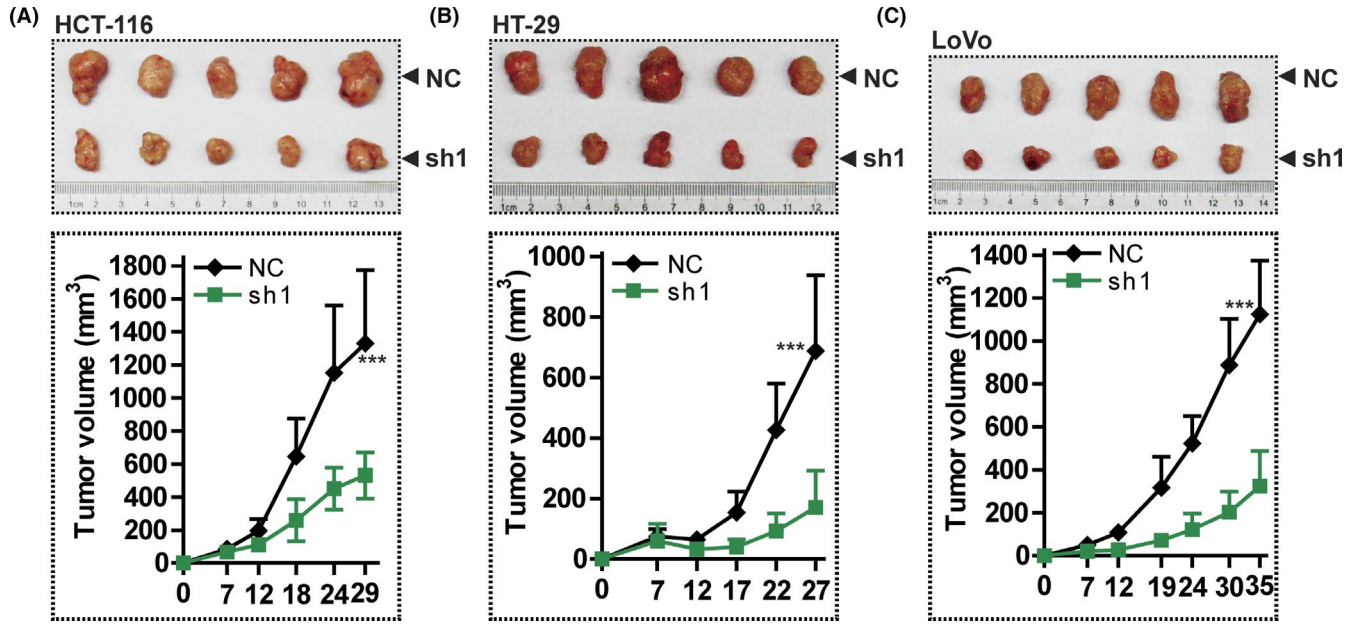

FIGURE 3 GPR126 knockdown attenuates colorectal cancer cell growth in vivo. A-C, GPR126 knockdown in HT-29, HCT116, and LoVo cells inhibited tumorigenesis in nude mice xenografts. Top panels, pictures of five representative tumors grown from each cell line. Bottom panels, statistical analysis of the volumes of 10 tumors formed from HCT-116 (A), 15 tumors from HT-29 (B), and eight tumors from LoVo (C). The volume curves were calculated on day 29 for HCT-116 tumors (A), day 27 for HT-29 (B), and day 35 for LoVo (C). Values are presented as the mean ± SEM. ***P <.001

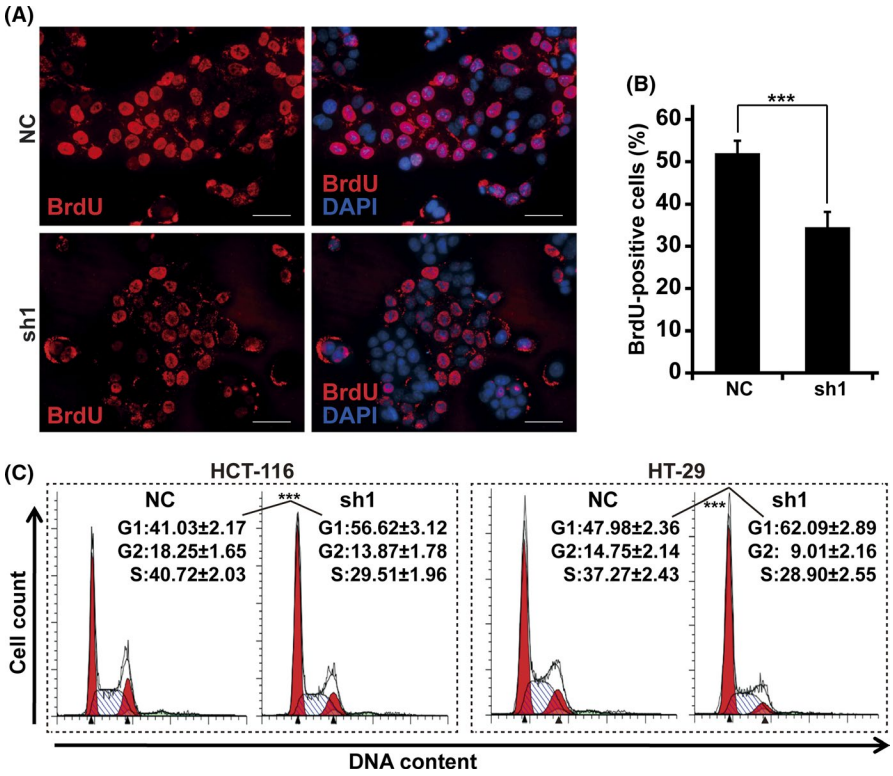

FIGURE 4 GPR126 knockdown leads to DNA synthesis inhibition and cell arrest in G1 phase in HT-29 and HCT-116 cells. A, B, Representative images of BrdU (red) and DAPI (blue) staining in NC- and GPR126-sh1-infected HT-29 cells; scale bars = 20 μm (A). Ratio of BrdU-positive cells to the total number of DAPI-positive cells; more than 10 fields were counted per group (B). C, Cell cycle analysis of NC- and GPR126-sh1-infected HCT-116 and HT-29 cells; three independent experiments were performed. The cell percentages in the G1, S, and G2 phases are indicated. Values are presented as the mean ± SEM. ***P <.001

of 88.81% and 81.19% using the NC- and GPR126-sh1 HT-29 cells, respectively (Figure S5). RNA-Seq analysis revealed that GPR126 knockdown down-regulated 1339 genes and up-regulated 668 genes in HT-29 cells. Bioinformatic analysis indicated that GPR126 knockdown mainly affected 15 signaling pathways, including DNA replication and cell cycle, in HT-29 cells (Figure 5A). Typical genes participating in DNA replication and cell cycle and were regulated by GPR126 knockdown in the RNA-Seq assay are shown in Figure 5B. RNA-Seq analysis also showed that levels of mRNAs encoding *S100A10*, *S100A9*, *SMO*, *BCL2*, *E2F2*, *HDAC2*, and *GLI2* were markedly decreased in GPR126-knockdown HT-29 cells; qRT-PCR analysis confirmed the GPR126-mediated regulation of *S100A10*, *S100A9*, *BCL2*, *E2F2*, *HDAC2*, *SMO*, and *GLI2* mRNA in HT-29 cells (Figure 5C). In addition, qRT-PCR analysis revealed that *GLI1* mRNA levels, but not those of *HDAC1* mRNA, were decreased in GPR126-silenced cells (Figure 5C). Changes in *GLI1* expression were not observed via RNA-Seq analysis, possibly due to the generally weak signal of *GLI1* in control cells.

Western blotting subsequently revealed that GPR126 knockdown decreased E2F2, HDAC2, and GLI2 expression but not that of HDAC1 and SIRT1 in HCT-116 and HT-29 cells (Figure 5D). Tumor tissues from xenograft models were also used to evaluate the effect of GPR126 knockdown on HDAC1, HDAC2, GLI1, and GLI2 expression. We found that HDAC2, GLI1, and GLI2 levels were decreased in GPR126-knockdown HCT-116 and HT-29 cells (Figure 5E). Considering that genes down-regulated by GPR126 knockdown, such as *SMO*, *GLI2*, *GLI1*, and *BCL2* (Figure 5C-E) are components of HH signaling, we theorized that GPR126 may regulate the HH signaling pathway in addition to mediating *E2F2*, *HDAC2*, *GLI1*, and *GLI2* expression in HCT-116 and HT-29 cells.

3.5 | GPR126 regulates colorectal cancer cell proliferation via HDAC2 and GLI2

Rescue experiments were performed to further investigate whether GPR126 knockdown-induced proliferation inhibition was due to HDAC2 down-regulation in HT-29 cells. Ectopic expression of HDAC2 in GPR126-silenced cells significantly restored HT-29 and HCT-116 cell viability (Figures 6A and S6A). Forced expression of HDAC2 cells also significantly restored the ratio of BrdU incorporation in GPR126-silenced HT-29 cells (Figure 6C,D). BrdU immunostaining of cells infected with GPR126 sh1 and empty overexpression vector (NC-Zs) showed 35% BrdU-positive cells, whereas forced expression of HDAC2 (Zs-HDAC2) in GPR126-sh1-HT-29 cells significantly increased the percentage to 46% (Figure 6D). Cell cycle analysis showed that *HDAC2* overexpression in GPR126-knockdown cells partially decreased the accumulation of HT-29 and HCT-116 cells in G1 phase (Figures 6E,F and S6B).

Western blotting showed that restored expression of HDAC2 in GPR126-silenced HT-29 cells also recovered GLI2 expression (Figure 6B). To eliminate the influence of GPR126 knockdown in HT-29 cells, we examined whether HDAC2 knockdown alone regulates GLI2 expression and found that it decreased GLI2 protein levels (Figure 7A). GLI2 is an acetylated protein whose HDAC-mediated deacetylation promotes transcriptional activation. In our chip assay, HDAC2 and GLI2 were found to bind to the PTCH1

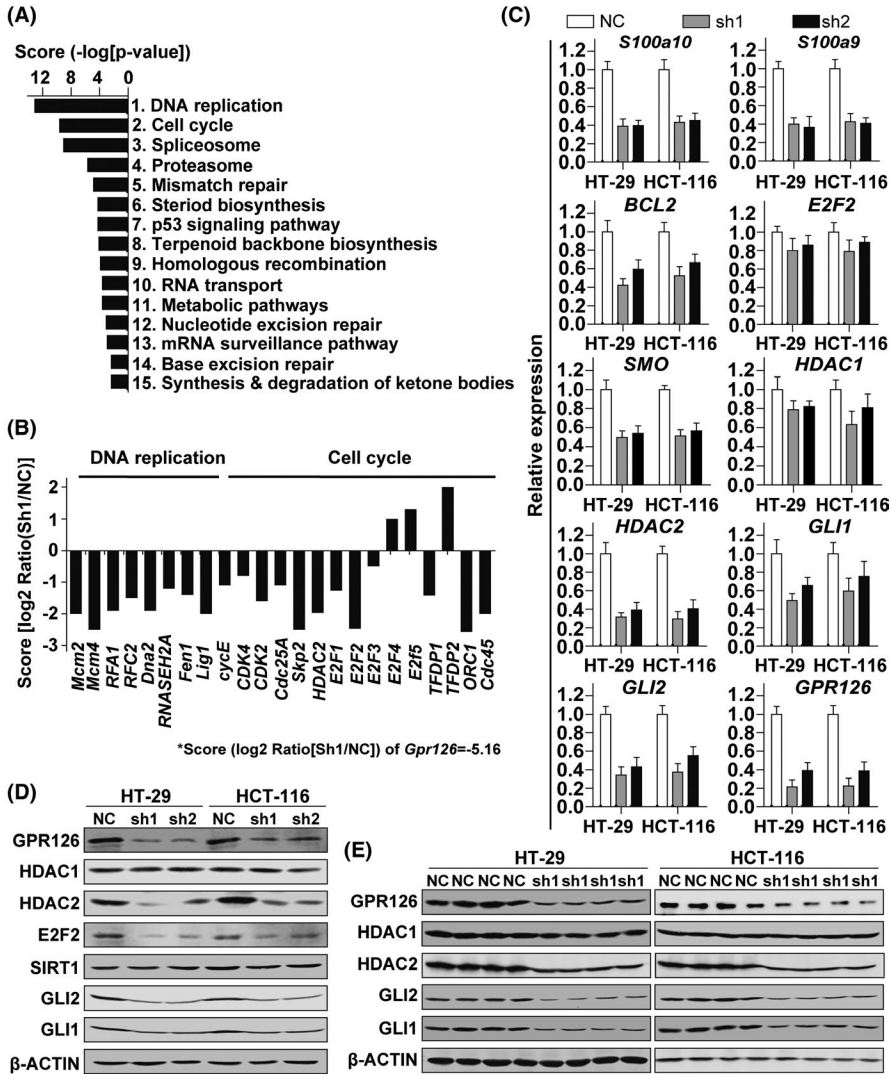

FIGURE 5 GPR126 knockdown decreases DNA synthesis and expression of cell cycle-related genes. A, Top 15 signaling pathways affected by GPR126 knockdown in gene ontology annotation analysis according to RNA-Seq. B, Representative genes regulated by GPR126 participating in DNA replication and cell cycle regulation in RNA-Seq. C, qRT-PCR, with the β-actin as the internal control was used to analyze mRNA levels of the indicated genes, which were found to be regulated by GPR126 via RNA-Seq. D, Western blotting of the indicated proteins in NC- and GPR126-sh1-infected HT-29 and HCT-116 cells. β-actin was used as loading control. E, Western blotting of the indicated proteins in HT-29- and HCT-116-xenograft tumors

promoter, indicating that HDAC2 also affects GLI2 transactivation activity in HT-29 cells (Figure 7B). A luciferase reporter assay was used to evaluate GPR126 and HDAC2 effects on the transcriptional activity of GLI2. The activity of GLI2 luciferase reporter (pGL3-GLI2-Luc) in GPR126 silenced HT-29 cells was significantly lower than that in vector control cells (Figure 7C). Ectopic expression of HDAC2 significantly restored the luciferase activity of pGL3-GLI2-Luc in GPR126 silenced HT-29 cells (Figure 7C). This result, combined with the previouse findings (Figure 6A-F) indicated that HDAC2 and GLI2 bind to the PTCH1 promoter (Figure 7B) and affect GLI2 transactivation activity in HT-29 cells (Figure 7C), indicating that GPR126 regulates GLI2 expression. HDAC2, as a GPR126 regulated protein, regulates GLI2 expression and could be a positive modulator of GLI2 (Figure 7F).

We further investigated the effect of purmorphamine as the hedgehog (HH) agonist[39] and GANT61[40] as an inhibitor of both Gli1 and Gli2, on the viability of vector control virus (NC) and GPR126 shRNA virus infected (sh1) colorectal cancer cells. Purmorphamine at doses of 2 and 4 μM significantly restored the cell viability and expression of GLI2 proteins in GPR126 shRNA virus-infected colorectal cancer cells (Figures 7D and S7A). GANT61 at 15 μM significantly decreased cell viability and GLI2 protein levels in both vector control virus (NC) and GPR126 shRNA virus (sh1) infected HT-29 cells (Figures 7E and S7B). Based on our findings (Figures 5, 6, and 7), we believe that GLI2, as a downstream component of the HH pathway, may be regulated by GPR126 in colorectal cancer cells.

Our findings indicate that GPR126 regulates colorectal cancer cell proliferation by mediating HDAC2 and GLI2 expression. HDAC2, a GPR126 regulated protein, regulates GLI2 expression and may be a positive modulator of the active members of the GLI family (Figure 7F).

4 | DISCUSSION

Colorectal cancer is one of the leading causes of cancer-related death worldwide.[41] Thus, investigating the development of colorectal cancer is important. Several genome analysis studies have revealed that GPR126 may play an important role in tumors, including breast cancer, bladder cancer, and acute myeloid leukemia.[13-19] In this study, GPR126 was found to regulate colorectal cancer cell

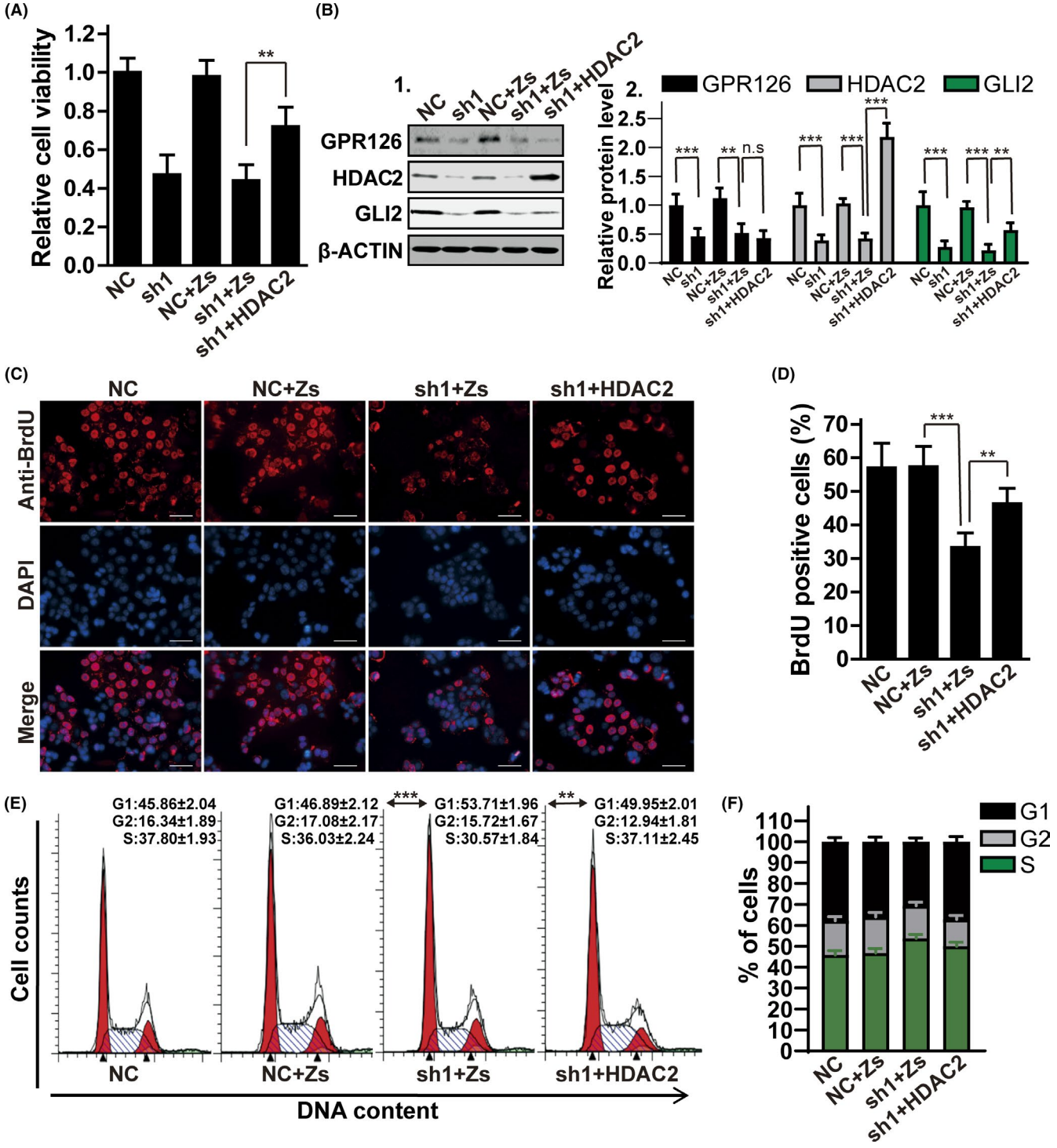

FIGURE 6 Ectopic expression of HDAC2 in GPR126-silenced cells restores cell viability, BrdU incorporation into DNA, and decreases cell accumulation in the G1 phase. A, B, Ectopic expression of HDAC2 in GPR126-silenced HT-29 cells. Relative cell viability (A) and western blotting of protein expression (B1) and the quantification of protein levels (B2) of the indicated groups. NC, cells infected with control vector; sh1, cells infected with GPR126 shRNA; NC + Zs, cells infected with control vector and empty overexpression control vector control (Zs); sh1 + Zs, cells infected with GPR126 shRNA and empty overexpression control vector control; sh1 + HDAC2, cells infected with GPR126 shRNA and HDAC2 overexpression vector. β-actin was used as loading control. C-F, Brdu incorporation assay and cell cycle analysis of ectopic expression of HDAC2 in GPR126-silenced HT-29 cells. Representative immunostaining images of BrdU (red) and DAPI (blue) staining of the indicated groups; scale bars = 20 μm (C). Ratio of BrdU-positive cells to the total number of DAPI-positive cells; more than 10 fields were counted per groups (D). Cell cycle analysis of the indicated groups in HT-29 cells (E) and the quantification of cell percentages in the G1, S, and G2 phases (F); three independent experiments were performed. Values are presented as the mean ± SEM. $^{**}P < .01$

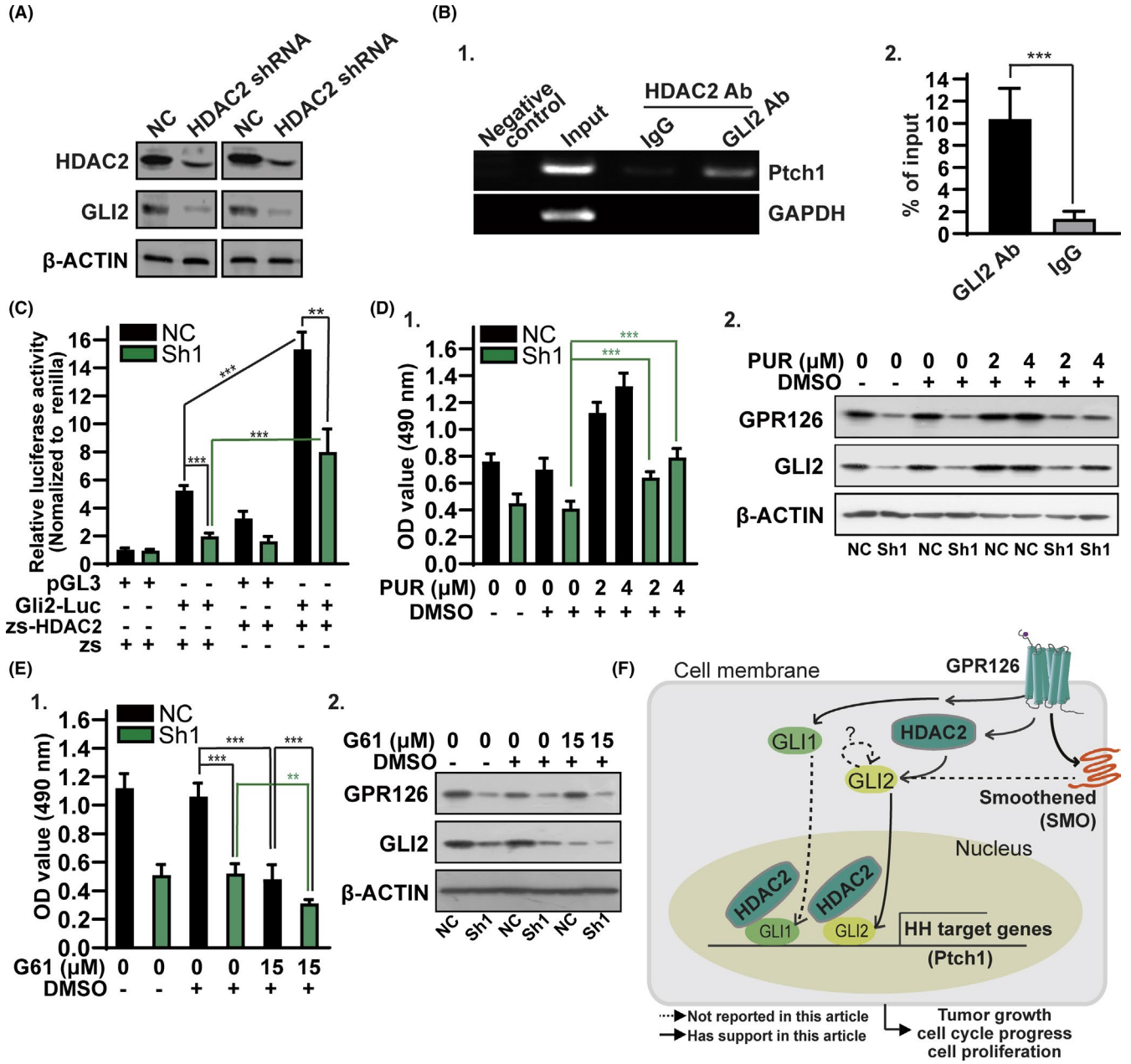

FIGURE 7 GLI2 binding with HDAC2 to the PTCH1 promoter is regulated by HDAC2 and its expression recovery restores cell viability in GPR126-silenced cells. A, Western blotting of HDAC2 and GLI2 protein levels in NC- and HDAC2-shRNA-infected HT-29 cells. β-actin was used as a loading control. B, Chromatin from HT-29 cells was immunoprecipitated with anti-HDAC2 antibodies and then eluted and immunoprecipitated again with normal mouse IgG(IgG) or anti-Gli2(GLI2 Ab). Eluted DNA was PCR-amplified using PTCH1 and GAPDH primers (B1). Quantitative PCR(qPCR) was used to examine the abundance of eluted DNA from B1, with the DNAs from input control as the internal control (B2). C, Ectopic expression of HDAC2 in GPR126-silenced cells restores transcription activity of GLI2 promoter (Gli2-Luc). NC or Sh1, cell infected by control virus or GPR126 shRNA virus; pGL3, empty luciferase vector; Gli2-Luc, luciferase vector with Gli2 promoter; zs-HDAC2, HDAC2 ectopic expression construct; zs, empty vector for cloning HDAC2 expression vector; '-', not used in co-transfection; '+', used in co-transfection. D, E, the effect of Purmorphamine (hedgehog agonist) and GANT61 (GLI2 inhibitor), at indicated concentration, on cell viability and GLI2 protein expression in indicate colorectal cancer cells. DMSO, the solvent of Purmorphamine and GANT61. β-actin was used as a loading control. F, Diagram illustrating the putative mechanisms of GPR126 function in colorectal cancer cells. GPR126 regulates SMO, GLI1, and HDAC2 expression (GSE106696). GLI1 and GLI2, as the downstream components of GPR126 signaling, regulate the expression of hedgehog (HH) target genes, including *PTCH1*, regulating tumor growth. HDAC2 is regulated by GPR126 regulated HDAC2, mediating GLI2 expression, and binds with GLI2 to the PTCH1 promoter or other promoters of HH target genes. The dotted line indicating 'Not reported in this article'; solid line indicating 'Has support in this article'; '?' meaning 'through unknown mechanism'

proliferation in vitro and in vivo, as well as GLI2 expression, by mediating HDAC2 expression. Our findings improve our understanding of the role of GPR126 in colorectal carcinogenesis.

GPR126 expression was increased in colorectal cancer tissues compared with matched adjacent mucosa samples and was highly enriched in nine colorectal cancer cell lines. GPR126 knockdown significantly inhibited HT-29 and HCT-116 cell proliferation and also inhibited the growth of HCT-8, HCT-15, and Caco-2 cells. Our findings are in agreement with another study, in which knockdown of GPR126 in SW780 and 5637 cells, which originate from urothelial bladder carcinomas, inhibited cell growth and compromised the ability to recruit human umbilical vein endothelial cells during tube formation.[17] Thus, in addition to promoting cell growth in endothelial cells,[4] GPR126 promotes tumor cell growth.

GPR126 was also implicated in the regulation of the HH signaling pathway in our study. Previously, *GPR126* knockout was found to regulate desert hedgehog (*Dhh*) and Indian hedgehog (*Ihh*), together with *SMO* and *GLI* family members—which are HH signaling components—on the mRNA level.[20,42] In our RNA-Seq (GSE106696) and qRT-PCR experiments, *SMO*, *GLI1*, and *GLI2* mRNA levels were significantly decreased in GPR126-knockdown HT-29 cells; GLI1 and GLI2 protein levels were also found to be decreased via western blotting. Given that GLI2 and GLI2 are the key transcriptional checkpoints of HH signaling,[26,43] we can assume that GPR126 regulates the HH signaling pathway in HT-29 and HCT-116 cells. We are also inclined to believe that there is cross-talk between GPR126-cAMP signaling and the HH signaling pathway, although the exact role of GPR126 in mammals remains unclear.[44] Because HH signaling is very important in the regulation of stem cell self-renewal, cell proliferation, and cell fate determination in both embryonic development and cancer tumorigenesis,[43,45] GPR126 signaling may participate in mammalian development and tumor progression by regulating HH signaling, which was partially supported by the finding that purmorphamine restored the cell viability and expression of GLI2 proteins in GPR126 shRNA virus infected HT-29 cells.

Finally, GPR126 was found to regulate transcription by influencing acetylation in cells. GPR126 regulated *HDAC2* but not *HDAC1* expression; further study should be conducted to uncover noncoding RNAs regulating the differential production of the HDACs within these cells. We further found that GLI2 directly bound to the promoter region of *PTCH1* is also bound to HDAC2 in HT-29 colorectal cells. In NIH3T3 cells, HDAC2 interacted with the GLI1 bound to the *PTCH* promoter, mediating HH-induced transcriptional activation. A previous luciferase reporter assay revealed that HDAC2 potentiates both basal and GLI1/GLI2-mediated transcription.[31] Our findings further support the notion that HDAC2 enhances HH-induced transcriptional activation. In our rescue experiment, we found that restored expression of HDAC2 in GPR126-silenced HT-29 cells also recovered GLI2 expression, and the activity of GLI2 luciferase reporter. Knockdown of HDAC2 also decreased GLI2 protein levels in HT-29 cells. These results suggest that there might be a positive feedback loop in which acetylated GLI2 regulates its own expression. Given that GPR126 signaling,[1,42] HH signaling,[46] and HDAC2[47] have been demonstrated to regulate myelination in the peripheral nervous system, it may be interesting to evaluate whether signal transduction mediated by GPR126-HDACs-HH is universal in mammals.[46]

Altogether, our findings demonstrate that GPR126 proteins play an important role in colorectal cancer cell proliferation by regulating GLI2 expression through HDAC2. These findings further emphasize the role of GPR126 in colorectal cancer and may assist in the development of drug screens for targeting GPR126 in tumors.

ACKNOWLEDGMENTS

This study was supported, in part, by the Science Fund for Research Initiation for Doctor of Second Affiliated Hospital of Nantong University, grants from the Nantong Municipal Bureau of Science and Technology (MS12020001), the Nantong Municipal Health and Family planning commission (M2020010), the National Natural Science Foundation of China (NO.81874140 and NO.81873555), Shanghai health and family planning commission (201740141) and Shanghai Municipal Commission of science and technology (19411966200).

CONFLICTS OF INTEREST

The authors have no conflict of interest.

ORCID

Hengxiang Cui https://orcid.org/0000-0002-1304-6134

REFERENCES

1. Monk KR, Naylor SG, Glenn TD, et al. A G protein-coupled receptor is essential for Schwann cells to initiate myelination. *Science*. 2009;325:1402-1405.
2. Mogha A, Harty BL, Carlin D, et al. Gpr126/Adgrg6 has Schwann cell autonomous and nonautonomous functions in peripheral nerve injury and repair. *J Neurosci*. 2016;36:12351-12367.
3. Glenn TD, Talbot WS. Analysis of Gpr126 function defines distinct mechanisms controlling the initiation and maturation of myelin. *Development*. 2013;140:3167-3175.
4. Ravenscroft G, Nolent F, Rajagopalan S, et al. Mutations of GPR126 are responsible for severe arthrogryposis multiplex congenita. *Am J Hum Genet*. 2015;96:955-961.
5. Cui H, Wang Y, Huang H, et al. GPR126 protein regulates developmental and pathological angiogenesis through modulation of VEGFR2 receptor signaling. *J Biol Chem*. 2014;289:34871-34885.
6. Waller-Evans H, Prömel S, Langenhan T, et al. The orphan adhesion-GPCR GPR126 is required for embryonic development in the mouse. *PLoS One*. 2010;5:e14047.
7. Patra C, van Amerongen MJ, Ghosh S, et al. Organ-specific function of adhesion G protein-coupled receptor GPR126 is domain-dependent. *Proc Natl Acad Sci USA*. 2013;110:16898-16903.
8. Diamantopoulou E, Baxendale S, de la Vega de León A, et al. Identification of compounds that rescue otic and myelination defects in the zebrafish adgrg6 (gpr126) mutant. *eLife*. 2019;8.
9. Sun P, He L, Jia K, et al. Regulation of body length and bone mass by Gpr126/Adgrg6. *Sci Adv*. 2020;6:eaaz0368.
10. Xu E, Shao W, Jiang H, et al. A genetic variant in GPR126 causing a decreased inclusion of exon 6 is associated with cartilage development in adolescent idiopathic scoliosis population. *BioMed Res Int*. 2019;2019:4678969.
11. Eichstaedt CA, Pagani L, Antao T, et al. Evidence of early-stage selection on EPAS1 and GPR126 genes in Andean high altitude populations. *Sci Rep*. 2017;7:13042.

12. Hosseini M, Fattahi Z, Abedini SS, et al. GPR126: a novel candidate gene implicated in autosomal recessive intellectual disability. *Am J Med Genet*. 2019;179:13-19.
13. Nik-Zainal S, Davies H, Staaf J, et al. Landscape of somatic mutations in 560 breast cancer whole-genome sequences. *Nature*. 2016;534:47-54.
14. Fatima A, Tariq F, Malik MFA, et al. Copy number profiling of MammaPrint genes reveals association with the prognosis of breast cancer patients. *J Breast Cancer*. 2017;20:246-253.
15. Shuai S, Drivers P, Functional Interpretation Working G, Gallinger S, Stein L, Consortium P. Combined burden and functional impact tests for cancer driver discovery using DriverPower. *Nature Comm*. 2020;11:734.
16. Garinet S, Pignot G, Vacher S, et al. High prevalence of a hotspot of noncoding somatic mutations in intron 6 of GPR126 in bladder cancer. *Mol Cancer Res*. 2019;17:469-475.
17. Wu S, Ou T, Xing N, et al. Whole-genome sequencing identifies ADGRG6 enhancer mutations and FRS2 duplications as angiogenesis-related drivers in bladder cancer. *Nature Comm*. 2019;10:720.
18. Xu S, Wang W, Xu C, et al. ROS1-ADGRG6: a case report of a novel ROS1 oncogenic fusion variant in lung adenocarcinoma and the response to crizotinib. *BMC Cancer*. 2019;19:769.
19. Maiga A, Lemieux S, Pabst C, et al. Transcriptome analysis of G protein-coupled receptors in distinct genetic subgroups of acute myeloid leukemia: identification of potential disease-specific targets. *Blood Cancer J*. 2016;6:e431.
20. Tang W, Zhou W, Xiang LI, et al. The p300/YY1/miR-500a-5p/HDAC2 signalling axis regulates cell proliferation in human colorectal cancer. *Nature Comm*. 2019;10:663.
21. Noh JH, Bae HJ, Eun JW, et al. HDAC2 provides a critical support to malignant progression of hepatocellular carcinoma through feedback control of mTORC1 and AKT. *Cancer Res*. 2014;74:1728-1738.
22. Gemoll T, Roblick UJ, Szymczak S, et al. HDAC2 and TXNL1 distinguish aneuploid from diploid colorectal cancers. *Cell Mol Life Sci*. 2011;68:3261-3274.
23. Huang BH, Laban M, Leung C h-w, et al. Inhibition of histone deacetylase 2 increases apoptosis and p21Cip1/WAF1 expression, independent of histone deacetylase 1. *Cell Death Diff*. 2005;12:395-404.
24. Zhu P, Martin E, Mengwasser J, et al. Induction of HDAC2 expression upon loss of APC in colorectal tumorigenesis. *Cancer Cell*. 2004;5:455-463.
25. Mazumdar T, DeVecchio J, Shi T, et al. Hedgehog signaling drives cellular survival in human colon carcinoma cells. *Cancer Res*. 2011;71:1092-1102.
26. Huang L, Walter V, Hayes DN, Onaitis M. Hedgehog-GLI signaling inhibition suppresses tumor growth in squamous lung cancer. *Clin Cancer Res*. 2014;20:1566-1575.
27. Ruiz i Altaba A, Mas C, Stecca B. The Gli code: an information nexus regulating cell fate, stemness and cancer. *Trends Cell Biol*. 2007;17:438-447.
28. Varnat F, Duquet A, Malerba M, et al. Human colon cancer epithelial cells harbour active HEDGEHOG-GLI signalling that is essential for tumour growth, recurrence, metastasis and stem cell survival and expansion. *EMBO Mol Med*. 2009;1:338-351.
29. Dauch P, Barelli H, Vincent JP, Checler F. Fluorimetric assay of the neurotensin-degrading metalloendopeptidase, endopeptidase 24.16. *Biochem J*. 1991;280(Pt 2):421-426.
30. Infante P, Alfonsi R, Botta B, et al. Targeting GLI factors to inhibit the Hedgehog pathway. *Trends Pharmacol Sci*. 2015;36:547-558.
31. Canettieri G, Di Marcotullio L, Greco A, et al. Histone deacetylase and Cullin3-REN(KCTD11) ubiquitin ligase interplay regulates Hedgehog signalling through Gli acetylation. *Nat Cell Biol*. 2010;12:132-142.
32. Cui H, Shao C, Liu Q, et al. Heparanase enhances nerve-growth-factor-induced PC12 cell neuritogenesis via the p38 MAPK pathway. *Biochem J*. 2011;440:273-282.
33. Kranenburg AR, de Boer WI, van Krieken JHJM, et al. Enhanced expression of fibroblast growth factors and receptor FGFR-1 during vascular remodeling in chronic obstructive pulmonary disease. *Am J Respir Cell Mol Biol*. 2002;27:517-525.
34. Fu J, Fong K, Bellacosa A, et al. VILIP-1 downregulation in non-small cell lung carcinomas: mechanisms and prediction of survival. *PLoS One*. 2008;3:e1698.
35. Jiang H, Wu P, Zhang S, et al. Global analysis of gene expression profiles in developing physic nut (Jatropha curcas L.) seeds. *PLoS One*. 2012;7:e36522.
36. Yu W, Qiu Z, Gao NA, et al. PAK1IP1, a ribosomal stress-induced nucleolar protein, regulates cell proliferation via the p53-MDM2 loop. *Nucleic Acids Res*. 2011;39:2234-2248.
37. Li D, Niu Z, Yu W, et al. SMYD1, the myogenic activator, is a direct target of serum response factor and myogenin. *Nucleic Acids Res*. 2009;37:7059-7071.
38. Dennler S, Andre J, Verrecchia F, Mauviel A. Cloning of the human GLI2 Promoter: transcriptional activation by transforming growth factor-beta via SMAD3/beta-catenin cooperation. *J Biol Chem*. 2009;284:31523-31531.
39. Wu X, Walker J, Zhang J, Ding S, Schultz PG. Purmorphamine induces osteogenesis by activation of the hedgehog signaling pathway. *Chem Biol*. 2004;11:1229-1238.
40. Yoshimoto AN, Bernardazzi C, Carneiro AJV, et al. Hedgehog pathway signaling regulates human colon carcinoma HT-29 epithelial cell line apoptosis and cytokine secretion. *PLoS One*. 2012;7:e45332.
41. Jemal A, Thomas A, Murray T, Thun M. Cancer statistics, 2002. *CA Cancer J Clin*. 2002;52:23-47.
42. Monk KR, Oshima K, Jors S, et al. Gpr126 is essential for peripheral nerve development and myelination in mammals. *Development*. 2011;138:2673-2680.
43. Kasper M, Schnidar H, Neill GW, et al. Selective modulation of Hedgehog/GLI target gene expression by epidermal growth factor signaling in human keratinocytes. *Mol Cell Biol*. 2006;26:6283-6298.
44. van den Brink GR, Bleuming SA, Hardwick JCH, et al. Indian Hedgehog is an antagonist of Wnt signaling in colonic epithelial cell differentiation. *Nat Genet*. 2004;36:277-282.
45. Ruiz i Altaba A, Sánchez P, Dahmane N. Gli and hedgehog in cancer: tumours, embryos and stem cells. *Nat Rev Cancer*. 2002;2:361-372.
46. Wu M, Hernandez M, Shen S, et al. Differential modulation of the oligodendrocyte transcriptome by sonic hedgehog and bone morphogenetic protein 4 via opposing effects on histone acetylation. *J Neurosci*. 2012;32:6651-6664.
47. Miller RH. Unwrapping HDAC1 and HDAC2 functions in Schwann cell myelination. *Nat Neurosci*. 2011;14:401-403.

SUPPORTING INFORMATION

Additional supporting information may be found online in the Supporting Information section.

How to cite this article: Cui H, Yu W, Yu M, et al. GPR126 regulates colorectal cancer cell proliferation by mediating HDAC2 and GLI2 expression. *Cancer Sci*. 2021;112:1798–1810. https://doi.org/10.1111/cas.14868